Accepted Manuscript

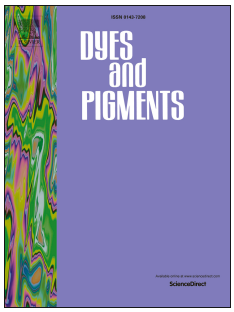

Luminescence properties of 2-benzoyl-1,3-indandione based EU^{3+} ternary and tetrakis complexes and their polymer films

Ilze Malina, Valdis Kampars, Sergey Belyakov

PII: S0143-7208(18)31203-8

DOI: 10.1016/j.dyepig.2018.07.003

Reference: DYPI 6857

To appear in: *Dyes and Pigments*

Received Date: 29 May 2018

Revised Date: 30 June 2018

Accepted Date: 2 July 2018

Please cite this article as: Malina I, Kampars V, Belyakov S, Luminescence properties of 2-benzoyl-1,3-indandione based EU^{3+} ternary and tetrakis complexes and their polymer films, *Dyes and Pigments* (2018), doi: 10.1016/j.dyepig.2018.07.003.

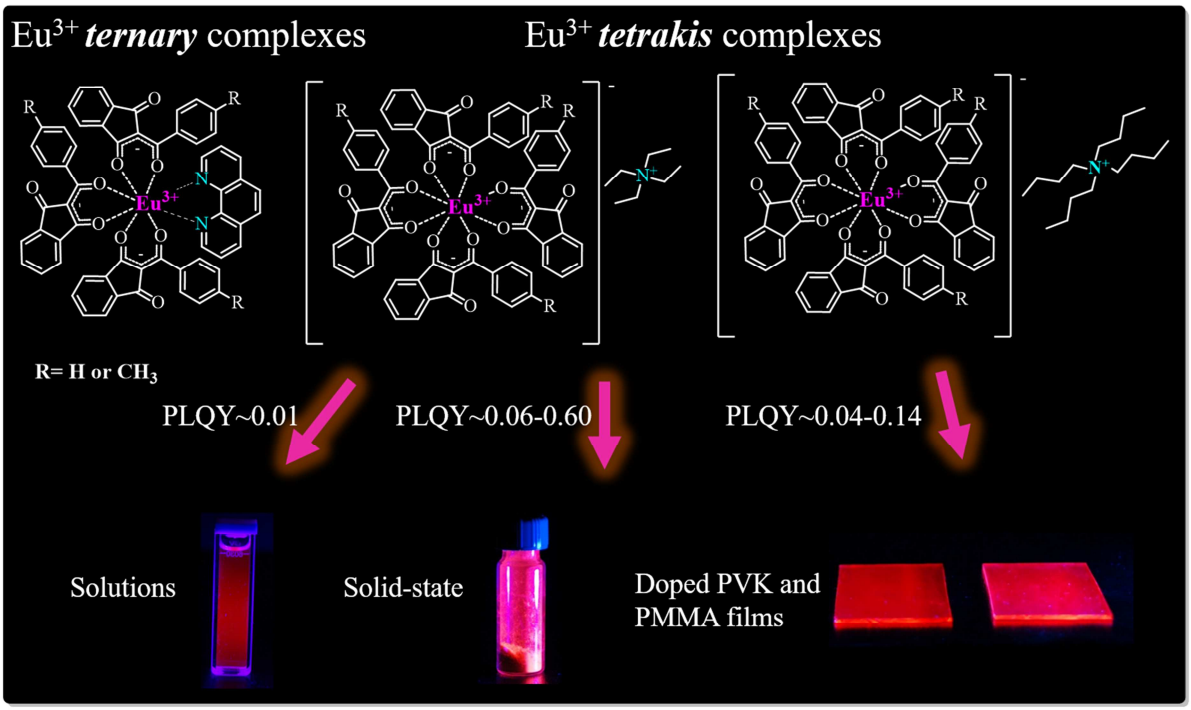

LUMINESCENCE PROPERTIES OF 2-BENZOYL-1,3-INDANDIONE BASED EU^{3+} TERNARY AND TETRAKIS COMPLEXES AND THEIR POLYMER FILMS

Ilze Malina[a,*], Valdis Kampars[a], Sergey Belyakov[a,b]

[a]*Riga Technical University, Institute of Applied Chemistry, Paula Valdena Str. 3, Riga, LV-1048, Latvia*
[b]*Latvian Institute of Organic Synthesis, Aizkraukles Str. 21, Riga, LV-1006, Latvia*

Abstract

Six new Europium(III) complexes with *ternary* and *tetrakis* structures - $Eu(BID)_3(PHEN)$, $Eu(MBID)_3(PHEN)$, $[Eu(BID)_4]^-N^+(Et)_4$, $[Eu(MBID)_4]^-N^+(Et)_4$, $[Eu(BID)_4]^-N^+(Bu)_4$, and $[Eu(MBID)_4]^-N^+(Bu)_4$ (BID – 2-benzoyl-1,3-indandionate, MBID - 2-(4-methylbenzoyl)-1,3-indandionate and PHEN – 1,10-phenantroline) are synthesized, characterized, and incorporated into poly-*N*-vinylcarbazole (PVK) and poly methyl methacrylate (PMMA) matrices. Complex structure shows significant effect on thermal properties and emission properties of complexes in solid-state. Used countercations ($N^+(Et)_4$ or $N^+(Bu)_4$) greatly affects complex solubility in solvents, absolute photoluminescence quantum yields and photoluminescence lifetimes in solid-state. Complexes exhibit red-light emission attributed to $^5D_0 \rightarrow {}^7F_J$ (J=0-4) transitions of Eu^{3+} ion with moderate to high quantum yields (0.06-0.60), bi-exponential lifetimes and pure red-light CIE chromaticity coordinates (x=0.670; y=0.330) in solid-state. Incorporation of synthesized complexes in PVK matrices leads to significant emission intensity and quantum yield decrease.

*corresponding author
E-mail adress: malina.ilze1@gmail.com or Ilze.Malina_1@rtu.lv (I.Malina)

However, doped PMMA films with synthesized complexes exhibit moderate PLQY (0.09-0.14) and longer lifetime values than in solid-state and could show potential application as polymer optical fibers or in OLED's and other devices.

Keywords: Europium; Tetrakis complex; Ternary complex; Luminescent polymer films.

1. INTRODUCTION

From all luminescent organic metal complexes with lanthanide ions (Ln^{3+}) trivalent Europium Eu^{3+} compounds stand out due to bright red-light emission with high quantum yields and long lifetimes. Popularity of Eu^{3+} complexes is so remarkable, that they have been investigated in wide range of fields and different type of materials, including nanoparticles for biomedical applications [1], mesoporous thin films for UV sensors and bio-sensing [2], as well as up-conversion luminescent thin films for wavelength-transfer imaging [3] and metal-organic framework microrods for colored optical waveguides [4] have been designed. Furthermore, due to noteworthy narrow emission line bandwidth, which defines the high red-light emission color purity, these compounds have been extensively investigated as emissive layers for organic/polymer light emitting diodes (OLEDs/PLEDs) [5].

To succeed with development of highly luminescent Eu^{3+} complexes one must deliberate the design of attached organic ligands. For effective excited energy transfer from ligands to Eu^{3+}, compatibility between energy levels of ligands and Eu^{3+} must be present in the complex. The main resonance level for Eu^{3+} is 17 250 cm^{-1} [6] and in order for complex to emit light, it is necessary that the triplet energy level of ligand is

close or even higher than this resonance level. Other just as important requirements for organic ligands are intense UV/Vis absorption, high chemical and thermal stability and simple, inexpensive synthesis. Till now the most popular class of organic compounds for Eu^{3+} chelating agents is β-diketones, which usually inherent above mentioned properties. However, structure of complex affects emission spectra profile and emission efficiency of Eu^{3+} ion as much as utilized ligands. Different structure of complexes can be obtained using different ratio of ligands to Eu^{3+} ion and utilization of secondary ligands. By using equimolar ratio of ligands to Eu^{3+} ion 3:1 the equimolar *tris*-complexes (Eu(β-diketone)$_3$) can be obtained, but usually, due to fact that coordination number of Eu^{3+} is 8 [7], complexes with general structure of Eu(β-diketone)$_3$(Solvent)$_2$ containing additional two solvent molecules are obtained instead. The coordination of these undesirable solvent molecules to Eu^{3+} ion can divert using secondary ligands - N- or O-donor containing compounds, such as 1,10-phenantroline (PHEN), therefore obtaining *ternary* complexes with general structure of Eu(β-diketone)$_3$(PHEN). It is possible to divert solvent molecules using fourth β-diketone ligand and obtain anionic *tetrakis* complexes [Eu(β-diketone)$_4$]$^-$, which can be stabilized with countercations, such as quaternary ammonium ions and alkali metal ions.

Till now literature data about Eu^{3+} organic complexes contains great amount of investigations about different ligand utilization for this lanthanide ion and their influence on emission properties. On the other hand, the data about comparison of different Eu^{3+} complex structure – *tris*, *ternary* and *tetrakis* effect on complex optical properties are documented poorly. Likewise, information about comparison of different countercation utilization in Eu^{3+} *tetrakis* complexes and their influence on the complex properties are limited [8, 9]. Therefore, for the first time comparison of

ternary and *tetrakis* complexes bearing the same β-diketone ligands are presented and full investigation about structure effect on thermal, absorption and emission properties are reported. Furthermore, two structurally similar counterions - tetraethylammonium and tetrabutylammonium cation are utilized in *tetrakis* complexes, therefore impact of counterion size on complex properties also are discussed. Lightly investigated rigid β-diketones - 2-benzoyl-1,3-indandione (HBID) and 2-(4-methylbenzoyl)-1,3-indandione (HMBID) with one carbonyl group in 1,3-indandione cycle are selected as ligands for Eu^{3+} complexes. Only few similar rigid binding ligands such as indone [10, 11] and 1,3-indandione [12, 13] derivatives have been reported so far as excellent chelating compounds for Eu^{3+} organic complexes. These type of compounds can magnify Eu^{3+} complex luminescence efficiency due to restriction of thermal vibration by rigid ligand, which leads to reduction of non-radiative deactivation of whole complex. Selected ligands exhibit not only easy synthesis and excellent solubility in commonly used solvents, but also high molar absorptivity. The synthesis of HBID and HMBID, and six new Eu^{3+} complexes with structures $Eu(BID)_3(PHEN)$, $Eu(MBID)_3(PHEN)$, $[Eu(BID)_4]^-N^+(Et)_4$, $[Eu(MBID)_4]^-N^+(Et)_4$, $[Eu(BID)_4]^-N^+(Bu)_4$ and $[Eu(MBID)_4]^-N^+(Bu)_4$ reported in this article are shown in Scheme 1. Characterization of complexes by ^{1}H-NMR and mass spectroscopy, FT-IR spectra, as well as X-Ray diffraction analysis are reported and optical properties in solutions and solid-state are investigated. Furthermore, different polymer thin films doped with complexes are obtained and their optical properties fully examined for practical evaluation of synthesized complexes in OLEDs.

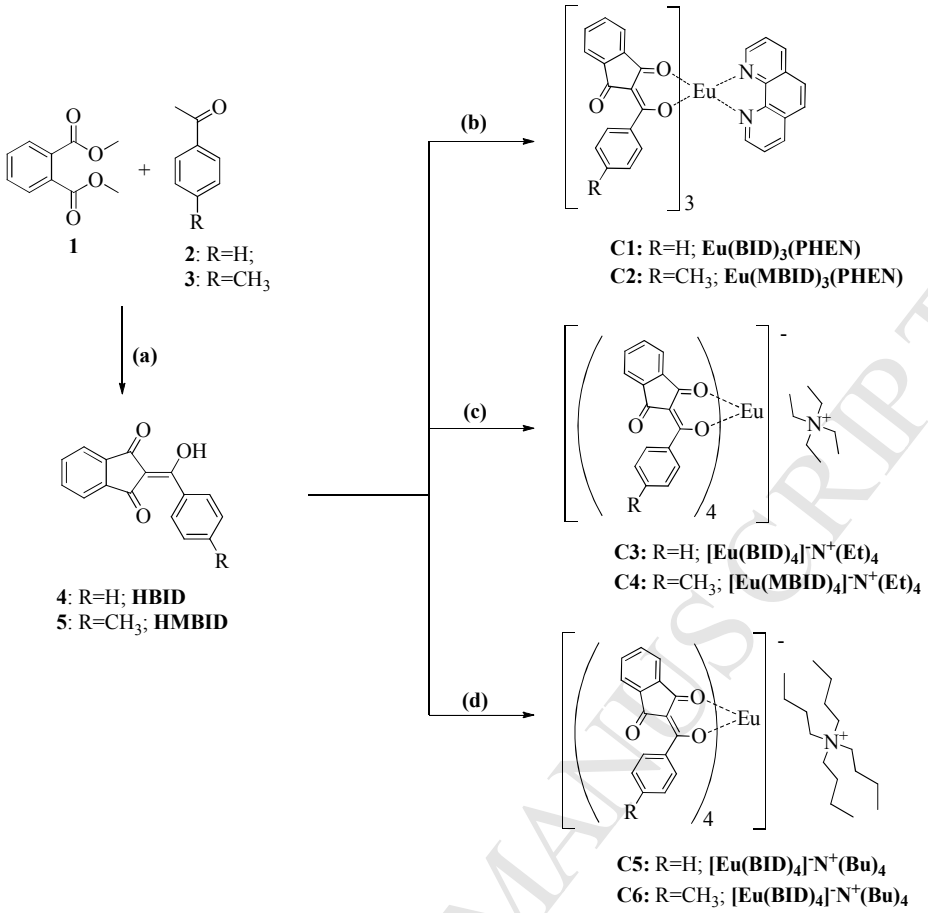

Scheme 1. Synthesis of complexes **C1**-**C6**; **(a) –** 1) $NaOCH_3$, toluene, 80 °C; 2) H_2O, 10% HCl; **(b)** – 10% NaOH/H_2O, 1,10-phenantroline, $EuCl_3 \cdot 6H_2O$; **(c)** – 10% NaOH/H_2O, $N(Et)_4Br$, $EuCl_3 \cdot 6H_2O$; **(d)** – 10% NaOH/H_2O, $N(Bu)_4Br$, $EuCl_3 \cdot 6H_2O$.

2. EXPERIMENTAL SECTION

2.1. Materials and instrumentation

$EuCl_3 \cdot 6H_2O$ (99.99%) and tetrabutylammonium bromide (98%), was purchased from *Acros Organics*, 1,10-phenantroline (99%), tetraethylammonium bromide (98%), acetophenone (96%) and 4-methylacetophenone (96%) were purchased from *Alfa Aesar*. Poly-*N*-vinylcarbazole (PVK) was purchased from *ABCR* (GmbH&Co), but poly(methyl methacrylate) (PMMA) from *Sigma Aldrich*. All substances were used without further purification. CHN elemental analyses were performed on Euro Vector EA 3000 analyzer. ^{1}H-NMR spectra were recorded in $CDCl_3$ or CD_3CN solutions (7 mg/ml) on a Brucker Avance 300 MHz spectrometer at 300 MHz for ^{1}H nuclei. Chemical shifts were expressed in parts per million (ppm)

relative to solvent signal. The FT-IR spectra (4000 to 650 cm^{-1}) were recorded on a Perkin-Elmer Spectrum 100 FTIR spectrometer using KBr pellets. Thermal properties were determined on a Perkin Elmer STA 6000 instrument. Each sample was heated from 30-890 °C with heating rate 10 °C/min in nitrogen atmosphere. The purity of synthesized ligands was established on Waters 2695 HPLC using Waters 2996 Photodiode array UV-Vis detector. The chromatographic analyses were performed using Xterra® MS C18 (5μm 2.1×100 mm) column, 50% Acetonitrile/0,1% formic acid solution as mobile phase and flow rate 0.2 ml/min. Low resolution mass spectra were acquired on a Waters EMD 1000MS mass detector (ESI+ mode, voltage 30 V). The UV/Vis absorption spectra were acquired using Perkin-Elmer 35 UV/Vis spectrometer, emission and excitation spectra were measured on QuantaMaster 40 steady state spectrofluorometer (Photon Technology International, Inc.). Absolute photoluminescence quantum yields were determined using QuantaMaster 40 steady state spectrofluorometer (Photon Technology International, Inc.) equipped with 6 inch integrating sphere by LabSphere. The lifetime measurements were carried out in room temperature using QuantaMaster 40 steady state spectrofluorometer equipped with high power Xenon flash lamp as excitation source. Polymer films were obtained with Laurell WS-400B-NPP/LITE spin coater. Diffraction data was collected on a Bruker-Nonius KappaCCD diffractometer using graphite monochromated Mo-Kα radiation (λ=0.71073 Å). The crystal structure was solved by direct methods [14] and refined by full-matrix least squares [15] using maXus complex of programs [16]. The crystal data, details of data collection and refinement are given in Table 1.

2.2. Fabrication of PVK and PMMA films

PVK or PMMA (20 mg) and complexes **C1-C6** (1.6 mg) were dissolved in 1 ml THF and the resulting mixture was heated at 40 °C for 0.5 h. Afterwards polymer

film was spin-coated on a glass substrate using following parameters: speed 800 rpm, acceleration 800 rpm/sec for 1 min. Then obtained films were dried in 60 °C for 2 h.

Table 1

Crystallographic data for complex **C4**.

Parameters	$[Eu(MBID)_4]^-N^+(Et)_4$
Formula	$C_{76}H_{64}EuNO_{12}$
Formula weight	1335.25
Wavelength	0.71073 Å
Crystal system	Monoclinic
Space group	C2/c
Unit cell dimensions	a = 27.2496(4) Å
	b = 16.0957(4) Å
	c = 20.2099(5) Å
α	90 deg
β	132.2274(10) deg
γ	90 deg
Volume	6563.7(2) $Å^3$
Z	4
Density (calculated)	1.351 g/cm^3
Absorption coefficient	1.019 mm^{-1}
F(000)	2744
Goodness-of-fit on F^2	1.861
Data / restraints / parameters	7778 / 0 / 407
Final R indices [I>2sigma(I)]	R1 = 0.1097, wR2 = 0.2783
R indices (all data)	R1 = 0.1301, wR2 =0.2859

2.3. Synthesis

The synthetic routes of compounds HBID and HMBID (**4**, **5**) and complexes **C1-C6** are shown in Scheme 1. 2-Benzoyl-1,3-indandione (**4**) and 2-(4-methylbenzoyl)-1,3-indandione (**5**) were synthesized as described in reference [13].

*2.3.1. Synthesis of ternary complexes **C1-C2***

C1 $Eu(BID)_3(PHEN)$: To a solution of 2-benzoyl-1,3-indandione (**4**) (1.08 mmol, 3 eq.) in 10 ml distilled water, which has been neutralized with 10% NaOH solution, an ethanol solution (5 ml) containing 1,10-phenantroline (0.36 mmol, 1 eq.) was added. The mixture was heated to 50 °C until complete dissolution of the compounds. Afterwards, obtained solution was added drop-wise to a 10 ml distilled water containing $EuCl_3 \cdot 6H_2O$ (0.36 mmol, 1 eq.). Instantly yellow precipitate was formed, which was allowed to stir for 4 hours in room temperature. Then, precipitate was

separated by suction filtration and crystalized from methanol solution and dried in vacuum at 50 °C for 24 hours. Yellow powder, Yield 41%; ^{1}H-NMR (300 MHz, $CDCl_3$, ppm): 10.03 (2H, d, H-PHEN), 9.41 (2H, br s, H-PHEN), 7.86-7.77 (4H, m, H-PHEN), 7.60-7.47 (6H, br m, H-1,3-Indand.), 6.83-6.80 (6H, br m, H-1,3-Indand.), 6.55 (6H, br s, H-Ph), 6.24 (3H, br s, H-Ph), 5.29 (6H, s, H-Ph); Anal. Calcd. For $EuC_{60}H_{35}N_2O_9$: C, 66.73; H, 3.24; N, 2.59; found C, 67.14; H, 3.55; N, 2.59; FT-IR (KBr, cm^{-1}): 3054 (ν_{Csp2H}); 1690, 1615 ($\nu_{C=O}$); 1586, 1566, 1519($\nu_{C=C}$); 1447 ($\nu_{C=N}$); ESI(+)-MS: (*m/z*) 181.2 $[PHEN+H]^+$; 899.6 $[^{151}Eu(2BID)_3+H]^+$; 901.4 $[^{153}Eu(2BID)_3+H]^+$.

C2 $Eu(MBID)_3(PHEN)$: Complex was synthesized by the same procedure as for **C1**, except 2-(4-methylbenzoyl)-1,3-indandione (**5**) was used instead of compound **4**. Yellow powder, Yield 31%; ^{1}H-NMR (300 MHz, $CDCl_3$, ppm): 10.02 (2H, d, H-PHEN), 9.43 (2H, br s, H-PHEN), 7.98-7.87 (4H, m, H-PHEN), 7.57-7.45 (6H, br m, H-1,3-Indand.), 6.84 (3H, br s, H-1,3-Indand.), 6.41-4.31 (9H, m, H-1,3-Indand., H-Ph), 5.27 (6H, br s, H-Ph), 2.24 (9H, s, Ph-CH_3); Anal. Calcd. For $EuC_{63}H_{41}N_2O_9$: C, 67.44; H, 3.66; N, 2.50; found C, 67.07; H, 3.82; N, 2.58; FT-IR (KBr, cm^{-1}): 3056, 3029 (ν_{Csp2H}); 2919, 2864 (ν_{Csp3H}); 1689, 1615 ($\nu_{C=O}$); 1584, 1563, 1512 ($\nu_{C=C}$); 1456 ($\nu_{C=N}$); ESI(+)-MS: (*m/z*) 181.1 $[PHEN+H]^+$; 941.6 $[^{151}Eu(MBID)_3+H]^+$; 943.4 $[^{153}Eu(MBID)_3+H]^+$.

*2.3.2. Synthesis of tetrakis complexes **C3-C6***

C3 $[Eu(BID)_4]^-N^+(Et)_4$: To a solution of 2-benzoyl-1,3-indandione (**4**) (1.08 mmol, 3 eq.) in 10 ml distilled water, which has been neutralized with 10% NaOH solution, distilled water solution (5 ml) containing tetraethylammonium bromide (0.54 mmol, 1.5 eq.) was added. The mixture was heated to 50 °C until complete dissolution of the

compounds. Afterwards, obtained solution was added drop-wise to a 10 ml distilled water containing $EuCl_3 \cdot 6H_2O$ (0.36 mmol, 1 eq.). Instantly yellow precipitate was formed, which was allowed to stir for 4 hours in room temperature. Then, precipitate was separated by suction filtration and crystalized from acetonitrile solution and dried in vacuum at 50 °C for 24 hours. Yellow powder, Yield 55%; ^{1}H-NMR (300 MHz, $CDCl_3$, ppm): 8.59 (4H, br s, H-1,3-Indand.), 7.70 (4H, br s, H-1,3-Indand.), 7.10 (8H, d, H-Ph), 6.78 (8H, m, H-1,3-Indand.), 6.46 (4H, br s, H-Ph), 5.96 (8H, br s, H-Ph), 4.27 (8H, br d, $(CH_3\text{-}C\underline{H_2})_4N^+$), 1.71 (12H, br s, $(C\underline{H_3}\text{-}CH_2)_4N^+$). Anal. Calcd. For $EuC_{72}H_{56}NO_{12}$: C, 67.61; H, 4.38; N, 1.10; found C, 67.44; H, 4.41; N, 1.30; FT-IR (KBr, cm^{-1}): 3083, 3054, 3018 (ν_{Csp2H}); 2997, 2977, 2948 (ν_{Csp3H}); 1681, 1619 ($\nu_{C=O}$); 1589, 1574, 1451 ($\nu_{C=C}$); 1266, 1212 ($\nu_{C\text{-}N}$); ESI(+)-MS: (*m/z*) 130.2 $[N(Et)_4]^+$; 899.4 $[^{151}Eu(BID)_3+H]^+$; 901.4 $[^{153}Eu(BID)_3+H]^+$.

C4 $[Eu(MBID)_4]^-N^+(Et)_4$: Complex was synthesized by the same procedure as for **C3**, except 2-(4-methylbenzoyl)-1,3-indandione (**5**) was used instead of compound **4**. Yellow crystals, Yield 44%; ^{1}H-NMR (300 MHz, CD_3CN, ppm): 8.31 (4H, H-1,3-Indand., d, *J*=9 Hz), 7.66 (4H, H-1,3-Indand., t, *J*=9 Hz), 7.11 (4H, H-1,3-Indand., t, *J*=9 Hz), 6.72 (8H, H-Ph, d, *J*=6 Hz), 6.35 (4H, H-1,3-Indand., d, *J*=9 Hz), 6.15 (8H, H-Ph, d, *J*=6 Hz), 3.17 (8H, q, $(CH_3\text{-}C\underline{H_2})_4N^+$), 2.30 (12H, s, Ph-$C\underline{H_3}$), 1.23 (12H, br t, $(C\underline{H_3}\text{-}CH_2)_4N^+$). Anal. Calcd. For $EuC_{76}H_{64}NO_{12}$: C, 68.37; H, 4.80; N, 1.05; found C, 67.53; H, 4.88; N, 1.09; FT-IR (KBr, cm^{-1}): 3019 (ν_{Csp2H}); 2924, 2802 (ν_{Csp3H}); 1679, 1615 ($\nu_{C=O}$); 1585, 1563, 1492, 1432 ($\nu_{C=C}$); 1284($\nu_{C\text{-}N}$); ESI(+)-MS: (*m/z*) 130.2 $[N(Et)_4]^+$; 941.6 $[^{151}Eu(MBID)_3+H]^+$; 943.4 $[^{153}Eu(MBID)_3+H]^+$.

C5 $[Eu(BID)_4]^-N^+(Bu)_4$: Complex was synthesized by the same procedure as for **C3**, except tetrabutylammonium bromide was used instead of tetraethylammonium

bromide. Yellow powder, Yield 50%; ^{1}H-NMR (300 MHz, $CDCl_3$, ppm): 7.02-6.87 (36H, m, H-1,3-Indand., H-Ph), 3.28 (8H, s, $(CH_3\text{-}CH_2\text{-}CH_2\text{-}C\underline{H_2})_4N^+$), 1.53 (8H, s, $(CH_3\text{-}CH_2\text{-}CH_2\text{-}C\underline{H_2})_4N^+$), 1.41 (8H, s, $(CH_3\text{-}CH_2\text{-}CH_2\text{-}C\underline{H_2})_4N^+$), 0.97 (12H, s, $(C\underline{H_3}\text{-}CH_2\text{-}CH_2\text{-}CH_2)_4N^+$). Anal. Calcd. For $EuC_{80}H_{72}NO_{12}$: C, 69.06; H, 5.18; N, 1.00; found C, 68.23; H, 4.99; N, 1.07; FT-IR (KBr, cm^{-1}): 3056 (ν_{Csp2H}); 2962, 2931, 2875 (ν_{Csp3H}); 1767, 1688 ($\nu_{C=O}$); 1621, 1588, 1574, 1568, 1492 ($\nu_{C=C}$); 1260 ($\nu_{C\text{-}N}$); ESI(+)-MS: (*m/z*) 242.4 $[N(Bu)_4]^+$; 899.5 $[^{151}Eu(2BID)_3+H]^+$; 901.5 $[^{153}Eu(2BID)_3+H]^+$.

C6 $[Eu(MBID)_4]^-N^+(Bu)_4$: Complex was synthesized by the same procedure as for **C3**, except 2-(4-methylbenzoyl)-1,3-indandione (**5**) was used instead of compound **4** and tetrabutylammonium bromide was used instead of tetraethylammonium bromide. Yellow powder, Yield 42%; ^{1}H-NMR (300 MHz, $CDCl_3$, ppm): 7.70-6.50 (32H, m, H-1,3-Indand., H-Ph), 4.02 (8H, br s, $(CH_3\text{-}CH_2\text{-}CH_2\text{-}C\underline{H_2})_4N^+$), 2.22 (12H, s, Ph-$C\underline{H_3}$), 1.99 (8H, br s, $(CH_3\text{-}CH_2\text{-}C\underline{H_2}\text{-}CH_2)_4N^+$), 1.72 (8H, br q, $(CH_3\text{-}C\underline{H_2}\text{-}CH_2\text{-}CH_2)_4N^+$), 1.12 (12H, t, $(C\underline{H_3}\text{-}CH_2\text{-}CH_2\text{-}CH_2)_4N^+$); Anal. Calcd. For $EuC_{84}H_{80}NO_{12}$: C, 69.71; H, 5.53; N, 0.97; found C, 69.19; H, 5.29; N, 1.00; FT-IR (KBr, cm^{-1}): 3034 (ν_{Csp2H}); 2960, 2876 (ν_{Csp3H}); 1739, 1683 ($\nu_{C=O}$); 1616, 1584, 1563, 1511, 1427 ($\nu_{C=C}$); 1282 ($\nu_{C\text{-}N}$); ESI(+)-MS: (*m/z*) 242.4 $[N(Bu)_4]^+$; 941.5 $[^{151}Eu(MBID)_3+H]^+$; 943.5 $[^{153}Eu(MBID)_3+H]^+$.

3. Results and Discussion

3.1. Characterization of Eu^{3+} complexes with BID and MBID ligands

To establish the structures of synthesized complexes – ^{1}H-NMR, mass spectroscopy, as well as element analysis and FT-IR spectroscopy were employed. Elemental analysis data were in a good agreement with proposed structures, but ^{1}H-

NMR spectroscopy was used to prove ratio of ligands in synthesized complexes. ^{1}H-NMR spectra of *tetrakis* complex **C3** is shown in Fig. 1. Due to the presence of paramagnetic metal ion – Eu^{3+} all proton signals are shifted to higher fields and shows peak broadening. In higher fields two signals corresponding to ethylene (8 protons, 4.25 ppm) and methyl (12 protons, 1.69 ppm) group protons from quaternary ammonium ion $N^{+}(Et)_4$ molecule were observed. Furthermore, at lower field six broad signals corresponding to 36 protons from four BID ligands were observed indicating, that in complex **C3** ratio of $N^{+}(Et)_4$ to BID is 1:4. Similar ^{1}H-NMR spectra were obtained for other *tetrakis* complexes **C4**-**C6**. Whereas in the ^{1}H-NMR spectra of *ternary* complexes **C1** and **C2** three signals at ~10.00, 9.40 and 7.90 ppm corresponding to eight protons from 1,10-phenantroline molecule were observed. Furthermore, in higher fields four broad signals corresponding to 27 protons from three BID ligands (**C1**) or five broad signals corresponding to 33 protons from three MBID ligands (**C2**) were obtained, which verifies that in these complexes ratio of PHEN:BID (or MBID) is 1:3.

Mass spectra of *ternary* complexes consists of three mass peaks, and for **C1** they are *m/z* 181.2 $[PHEN+H]^{+}$, 899.6 $[^{151}Eu(BID)_3+H]^{+}$ and 901.4 $[^{153}Eu(BID)_3+H]^{+}$ establishing, that Eu^{3+} and BID ratio in complex is 1:3. Unfortunately, molar masses of ions of *tetrakis* complexes ($[Eu(BID)_4]^{-}$ or $[Eu(MBID)_4]^{-}$) were over the mass spectra detection limit and only *tris* ions ($[Eu(BID)_3+H]^{+}$ or $[Eu(MBID)_3+H]^{+}$) and quaternary ammonium ions (*m/z* 242.4 $[N(Bu)_4]^{+}$ or 130.2 $[N(Et)_4]^{+}$) were detected.

In the FT-IR spectra of complexes **C1**-**C6** absence of any broad band around 3500 cm^{-1} (ν_{OH}) indicates, that they are anhydrous and there are no solvent molecules in Eu^{3+} coordination sphere. Furthermore, comparing complexes with BID ligands: *ternary* **C1** with *tetrakis* **C3** and **C5**, the latter two shows vibrations of $C_{sp3}H$ groups

from $N^+(Et)_4$ or $N^+(Bu)_4$ ions in the range from 2800-3000 cm^{-1}, verifying that these complexes are with *tetrakis* structure. Furthermore, compound FT-IR spectra of HBID (**4**) contains sharp peak at 1713 cm^{-1} and one at 1644 cm^{-1} corresponding to symmetric and asymmetric stretching vibrations of carbonyl group ($\nu_{C=O}$). In the FT-IR spectra of complexes **C1**, **C3** and **C5** both of these peaks appears on lower frequencies (for 22-32 cm^{-1}). Similar observations were reported for other 2-acyl-1,3-indandione complexes [17].

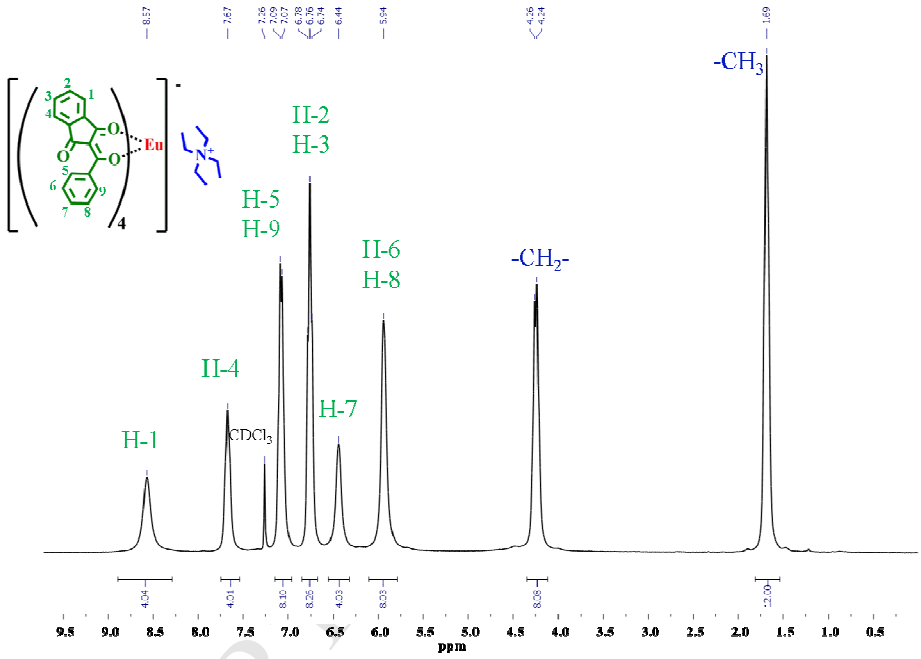

Fig. 1. ^{1}H-NMR spectra of *tetrakis* complex **C3** in $CDCl_3$ at 298 K.

Ternary complexes **C1** and **C2** and *tetrakis* complexes **C5** and **C6** with $N^+(Bu)_4$ cation shows excellent solubility in CH_2Cl_2, $CHCl_3$, THF, MeOH and MeCN. However, *tetrakis* complexes **C3** with $N^+(Et)_4$ cation exhibit slightly lower dissolution ability in commonly used solvents and **C4** is insoluble in non-polar solvents, but soluble in MeCN. It seems that, solubility of *tetrakis* complexes are mainly affected by used counterion ($N^+(Et)_4$ or $N^+(Bu)_4$) and complexes with $N^+(Bu)_4$ cation shows higher dissolution ability in polar and non-polar solvents.

3.2. Crystal structure of complex C4

Crystal of complex **C4** was obtained by slow evaporation of MeCN solution. X-ray structure of complex **C4** is shown in Fig. 2 (**A**) and selected bond lengths and angles are given in Table 2. Important disorder contribution has been encountered in these Eu complex crystals. *Tetrakis* complex $[Eu(MBID)_4]^-N^+(Et)_4$ **C4** crystallizes in the monoclinic space group *C*2/*c*. In the crystal structure both cations and anions lie on twofold symmetry axes. Therefore, the structure of the molecular ions consists of two parts with identical bond length and angles. No MeCN molecules were found trapped in crystal packing of **C4**.

Table 2

Selected bond lengths (Å) and angles (°) for complex $[Eu(MBID)_4]^-N^+(Et)_4$ **C4**.

Bond lengths				Bond angles	
Bond	Value, Å	Bond	Value, Å	Bond angle	Value, °
Eu(1)-O(4)	2.410(6)	Eu(1)-O(4)	2.410(6)	O(4)-Eu(1)-O(5)	72.40(19)
Eu(1)-O(5)	2.375(6)	Eu(1)-O(5)	2.375(6)	O(4)-Eu(1)-O(5)	72.40(19)
Eu(1)-O(6)	2.410(6)	Eu(1)-O(6)	2.410(6)	O(6)-Eu(1)-O(7)	72.30(2)
Eu(1)-O(7)	2.378(6)	Eu(1)-O(7)	2.379(6)	O(6)-Eu(1)-O(7)	72.30(2)

In the structure of complex **C4** each Eu^{3+} ion is coordinated with eight oxygen atoms from four β-diketone moieties. The mean bond length of Eu-O is 2.390 Å, which is a close value to other previously reported Eu-O bond lengths of Eu^{3+} *tetrakis* complexes with β-diketone ligands [17, 18, 19]. Furthermore, mean bond angle around central metal atom (O-Eu-O, where both oxygen atoms are from one β-diketone molecule) is 72.35 °, which is very close to reported value (72.23 °) for other Eu^{3+} complex with 2-acyl-1,3-indandionate ligands [13]. The geometrical arrangement of oxygen atoms in the first coordination sphere of Eu^{3+} ion can be described as trigondodecahedron (see Fig. 2 (**B**)).

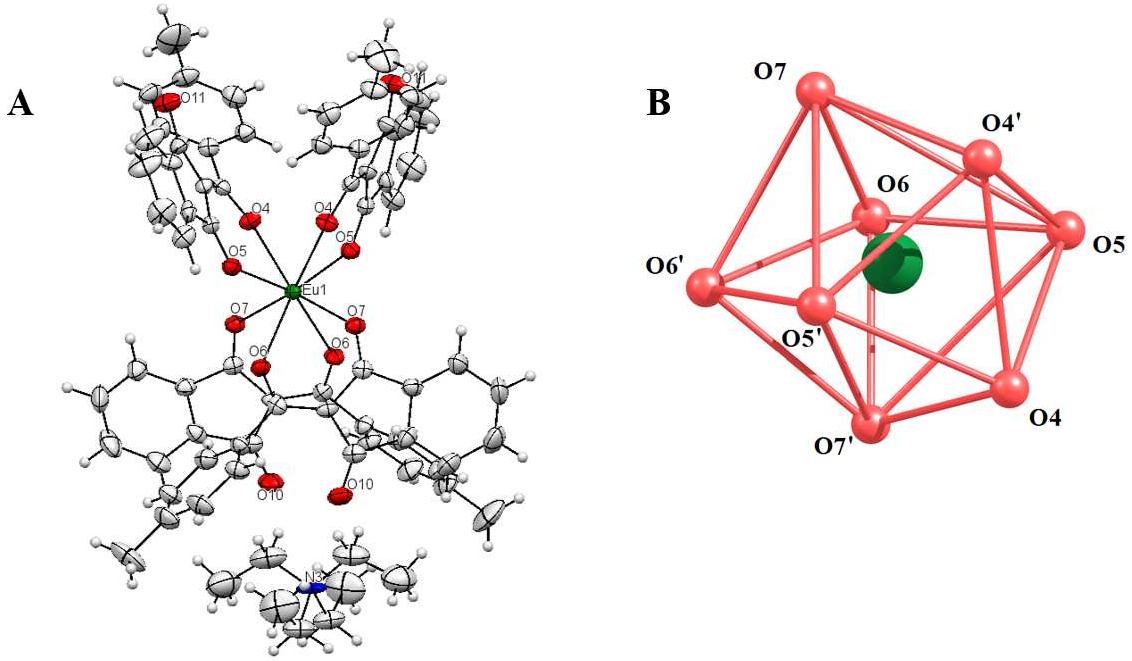

Fig. 2. (**A**) - X-Ray structure with 50% probability ellipsoids of crystal **C4** ($[Eu(MBID)_4]^-N^+(Et)_4$); (**B**) - Coordination polyhedron of europium in **C4**.

3.3. Thermal properties of Eu^{3+} complexes with BID and MBID ligands

The high thermal stability is necessary for practical application of organic luminescent materials in optoelectronic devices. Therefore, thermal stability of Eu^{3+} complexes was examined by thermogravimetric analysis (TGA) in the inert atmosphere and obtained thermal decomposition temperatures T_d are depicted in Table 3. TGA shows that the starting decomposition temperatures of *ternary* complexes **C1** and **C2** are 240 and 247 °C, respectively, and are lower than ones for *tetrakis* complexes **C3-C6** (299-307 °C). It seems, that introduction of secondary ligand PHEN in Eu^{3+} ion coordination sphere leads to reduction of T_d and can be explained with lower thermal stability of PHEN (start of T_d~240 °C) [21] than used β-diketonates BID and MBID. However, obtained T_d values for **C1** and **C2** are close to other previously reported destruction temperatures of Eu^{3+} *ternary* complexes with rigid β-diketone ligands [11]. On the other hand, for *tetrakis* complexes **C3-C6** thermal decomposition temperatures are higher by 52-67 °C. Moreover,

decomposition temperatures of *tetrakis* complexes is not influenced by used counterion ($N^+(Et)_4$ or $N^+(Bu)_4$) and obtained T_d values differs for only 3-5 °C. It can be concluded that synthesized *tetrakis* complexes exhibit ones of the highest thermal stabilities from currently reported *tetrakis* Eu^{3+} β-diketone complexes [19, 22], which usually do not exceed 300 °C.

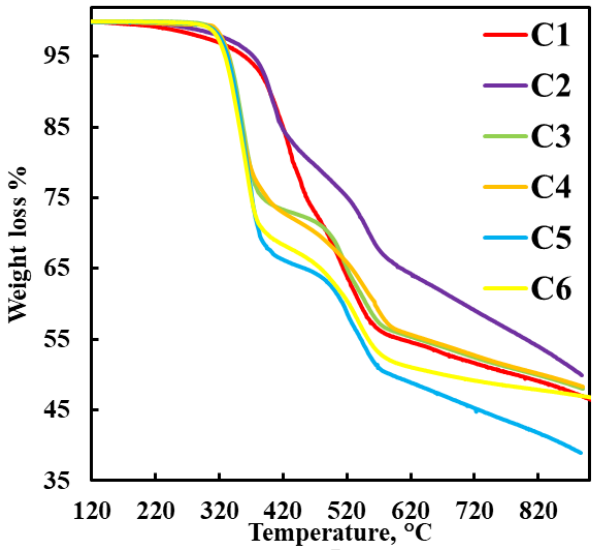

Fig. 3. TG curves of Eu^{3+} complexes **C1**-**C6** obtained in the nitrogen atmosphere with heating rate of 10 °C/min.

Destruction pattern of complexes was studied through obtained termogramms (Fig. 3). Termogramms of *ternary* complexes **C1** and **C2** consists of two rapid weight losses in the steps around 240-452, 453-570 °C (**C1**) and 247-426, and 427-580 °C (**C2**), which corresponds to the loss of organic ligands - one PHEN and one BID or MBID molecule. Further destruction of complex has followed by complicated decomposition and carbonization reactions, which lead to rather high residual weight – 46% and 49%, respectively. Similarly, *tetrakis* complexes **C3**-**C6** exhibits two rapid weight loss stages in TGA curve, and for complex **C5** they are at 299-410, 411-572 °C. The first stage can be signed to loss of counterion ($N^+(Bu)_4$) and one MBID molecule and second stage – to one MBID molecule. Similar destruction pattern was reported for *tetrakis* Eu^{3+} complexes with dibenzoylmethane ligands and

hexadecyltrimethyl ammonium or octadecyltriethyl ammonium counterions [23]. In the end of TGA (at 890 °C) high residual weight of *tetrakis* complexes (40-48%) are obtained similarly than for *ternary* complexes. Solid residue of all complexes was analyzed by CHN elemental analysis, and for complex **C6** it showed C, 65.31; H, 0.85; N, <0.30, which points to formation of solid residue with high fracture of carbon. Probably in high temperatures carbonization reactions takes place with remaining β-diketone ligands and remaining europium forms different inorganic compounds, for example Eu_2O_3. All obtained complexes exhibits proper thermal decomposition temperatures for application in the electronic devices.

3.4. UV/Vis absorption properties of Eu^{3+} complexes with BID and MBID ligands

UV/Vis absorption spectra of compounds HBID, HMBID, PHEN and their Eu^{3+} complexes were recorded in MeCN solutions (c~$1.5\cdot10^{-5}$M), also $EuCl_3\cdot6H_2O$ (c~$1.0\cdot10^{-3}$M) and Na complexes with BID and MBID ligands (Na(BID), Na(MBID)) (c~$1.5\cdot10^{-5}$M) were measured in EtOH solutions. Spectra of $EuCl_3\cdot6H_2O$, PHEN, HBID and its Na and Eu^{3+} complexes are shown in Fig. 4. $EuCl_3\cdot6H_2O$ dissolved in EtOH exhibits very weak absorption in UV light region, however secondary ligand PHEN shows intense absorption below 300 nm, with maximum at 290 nm (ε~50881 $M^{-1}\cdot cm^{-1}$). Compounds HBID and HMBID exhibit broad UV-light absorption between 275-400 nm with maximums at 297 and 331 for HBID and 299 and 336 nm for HMBID. Absorption at 297 and 299 nm attributes to π→π* transitions in 1,3-indandione, however lower energy bands corresponds to π→π* enolic transitions from β-diketone fragment [11]. Substituent ($-CH_3$) in benzoyl fragment has negligible effect on absorption maximum, and for HMBID $\lambda_{abs\ max}$ is shifted for 5 nm, compared to HBID $\lambda_{abs\ max}$. Molar absorptivity ε are 25625 (HBID) and 24306 (HMBID) M^{-}

^{1}·cm^{-1}, respectively. Furthermore, solutions containing Na complexes Na(BID) and Na(MBID) exhibits the same absorption profile as compounds HBID and HMBID with small blue-shift of $\lambda_{abs\ max}$ (2 nm). Similar observations, that Na complexes with rigid β-diketones exhibit almost identical absorption spectra as free ligands were reported previously [10, 11].

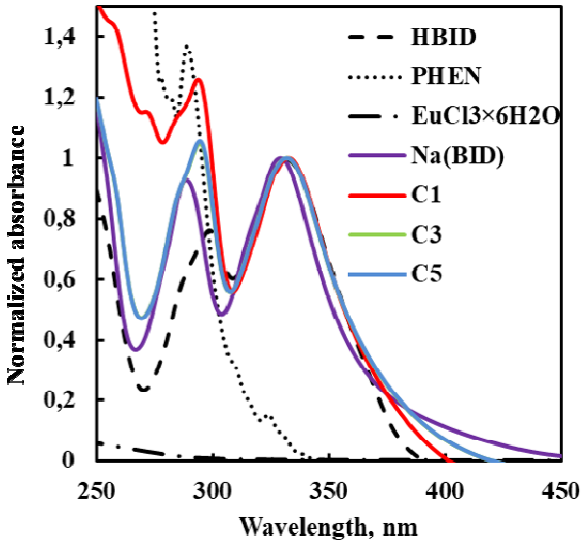

Fig. 4. UV/Vis absorption spectra of compounds HBID, PHEN, and Eu^{3+} complexes **C1**, **C3**, **C5** in MeCN solutions (c~1.5·10^{-5}M) and $EuCl_3·6H_2O$ (c~1.0·10^{-3}M) and Na complex with BID ligand Na(BID) (c~1.5·10^{-5}M) in EtOH solutions.

Furthermore, coordination with Eu^{3+} ion leads to some changes in UV/Vis spectra. MeCN solutions containing *ternary* complexes **C1** and **C2** exhibit absorption at region 250-294 nm, which attributes to the absorption of secondary ligand PHEN. However, lower energy bands location are not noticeably influenced by the presence of lanthanide ion and $\lambda_{abs\ max}$ lies at 332 nm for **C1** and 333 nm for **C2**. Molar absorptivity for complexes **C1**,**C2** as expected are considerably higher (ε ~56385 and 56131 M^{-1}·cm^{-1}) than for free ligands confirming fact, that complexes contains several ligands in their structures. MeCN solutions containing *tetrakis* complexes **C3**-**C6** shows exact absorption band shape as HBID and HMBID and since used countercations ($N^{+}(Et)_4$ and $N^{+}(Bu)_4$) does not exhibit absorption in 250-400 nm

range, the absorption bands for pairs **C3** and **C5**, and **C4** and **C6** even overlaps with each other. Similarly to *ternary* complexes, $\lambda_{abs\ max}$ for solutions containing *tetrakis* complexes differs from HBID and HMBID for 1-2 nm, but ε coefficients are in the range from 92370 to 94007 $M^{-1} \cdot cm^{-1}$. It can be concluded, that absorption spectra patterns of the solutions containing complexes **C1**-**C6** are almost identical to the ones observed for compounds HBID and HMBID, suggesting that coordination with Eu^{3+} ion shows negligible effect on $\pi \rightarrow \pi^*$ transitions of the ligands. Similar conclusions were reported for other *ternary* and *tetrakis* Eu^{3+} complexes with β-diketone ligands [10, 18, 22, 24].

3.5. Photoluminescence properties of Eu^{3+} complexes

Photoluminescence properties of synthesized complexes were investigated in MeCN solutions and solid-state through excitation and emission spectra. Excitation spectra (monitored at Eu^{3+} emission at 611 nm) of MeCN solutions ($c \sim 1.5 \cdot 10^{-5}$M) containing complexes **C1**-**C6** exhibits broad bands ranging from 300 to 440 nm (Fig. 5. (**A**)) with λ_{exc} at ~350 nm, which attributes to $\pi \rightarrow \pi^*$ transitions of coordinated ligands BID and MBID. Excitation bands match very well with absorption spectra of corresponding complexes, therefore confirming fact, that Eu^{3+} emission arise from energy absorbed by coordinated BID or MBID ligands. Furthermore, excitation spectra of *ternary* complexes **C1** and **C2** does not exhibit bands below 300 nm, where the secondary ligand PHEN absorbs the light, meaning that direct energy transfer from PHEN to Eu^{3+} ion is not present in these complexes.

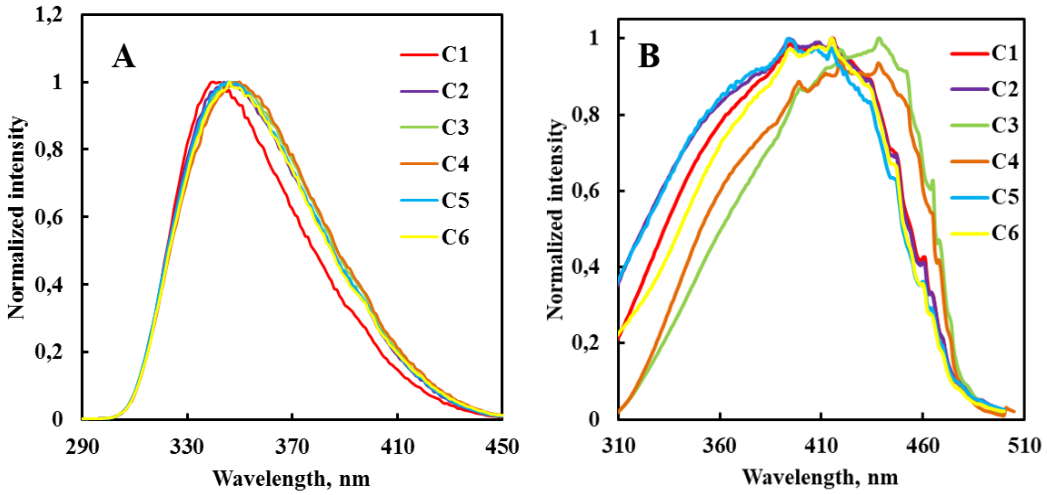

Fig. 5. (**A**) - Excitation spectra (λ_{mon}=611 nm) of Eu^{3+} complexes **C1**- **C6** in MeCN solutions (c~1.5·10^{-5}M); (**B**) - Excitation spectra (λ_{mon}=611 nm) of complexes **C1**-**C6** in solid-state.

Excitation spectra of complexes in solid-state (Fig. 5. (**B**)) contains much broader bands in 300-480 nm range with maximums at 408 nm for complexes **C1**,**C2**,**C5**,**C6**, and 425 nm for *tetrakis* complexes **C3** and **C4** with $N^{+}(Et)_4$ counterion. Such red shift of λ_{exc} in solid-state compared to solutions spectra is common for Eu^{3+} β-diketone complexes [18] and explained with the presence of strong π-π interactions between ligands in the solid-state. Furthermore, solid-state excitation spectra of **C1**-**C6** contains some of Eu^{3+} ion sharp absorption lines of *f*-*f** transitions at 394, 415 and 465 nm. However, these transitions are almost completely overlapped with excitation bands of complexes, therefore confirming, that excitation of Eu^{3+} ion through attached organic ligands is more efficient than direct excitation of Eu^{3+} absorption bands. In conclusion, excitation window for all six complexes in solid-state has been extended to the visible region (up to 480 nm), which is favorable property for Eu^{3+} complexes, due to frequently observed low stability of β-diketones in UV light.

Table 3

Thermal decomposition temperatures (T_d), absolute photoluminescence quantum yields (PLQY) and CIE coordinates calculated from emission spectra of complexes **C1**-**C6** in MeCN solutions (c~1.5·10^{-5}M) and in solid-state, luminescence lifetime (τ_1 and τ_2) of complexes **C1**-**C6** in solid-state.

	In MeCN solutions				In solid-state		
	PLQY	CIE 1931 coordinates x;y	τ_1, µs	τ_2, µs	PLQY	CIE 1931 coordinates x;y	T_d, °C
C1	<0.01	0.669; 0.331	121 ±4 (6%)	42±1 (94%)	0.06	0.670; 0.330	240
C2	<0.01	0.669; 0.331	122±3 (5%)	39±1 (95%)	0.10	0.670; 0.330	247
C3	0.01	0.669; 0.331	233±2 (22%)	54±1 (78%)	0.29	0.673; 0.329	302
C4	0.01	0.668; 0.331	203±17 (25%)	118±5 (75%)	0.60	0.673; 0.327	307
C5	0.01	0.669; 0.331	118 ±4 (4%)	37±1 (96%)	0.12	0.670; 0.330	299
C6	0.01	0.669; 0.331	115±6 (2%)	34±1 (98%)	0.11	0.670; 0.330	302

Emission of complexes **C1**-**C6** was investigated in MeCN solutions and solid-state, but due to fact, that emission profile is identical for complexes with similar structure (*ternary* or *tetrakis*) only one *ternary* complex **C2** and one *tetrakis* complex **C3** emission spectra are shown as examples (Fig. 6). In MeCN solutions, when excited with 350 nm, complexes exhibit weak red-light emission with characteristic Eu^{3+} ion narrow emission bands, which lies at 580, 594, 611, 652 and 701 nm and attributes to $^5D_0 \rightarrow {}^7F_J$ (J=0-4) transitions. Analogue, but more intense emission spectra profiles were obtained for complexes in solid-state, when excited with 408 or 425 nm. Commonly reported observations in the literature about emission profile of Eu^{3+} β-diketone complexes are also present for our newly synthesized complexes **C1**-**C6**: Emission bands at 580 and 652 nm shows weak intensity due to fact, that their corresponding transitions ($^5D_0 \rightarrow {}^7F_0$, $^5D_0 \rightarrow {}^7F_3$) are forbidden by electric dipole and magnetic dipole moments. Furthermore, transition $^5D_0 \rightarrow {}^7F_1$ (594 nm) is forbidden by electric dipole moment, but allowed by magnetic dipole moment and is almost insensitive from coordination environment around Eu^{3+} ion. This transition shows splitting (Inset, Fig. 6). Moreover, band at 611 nm ($^5D_0 \rightarrow {}^7F_2$) is hypersensitive

transition, which exhibit the highest intensity and is giving the red emission color for complexes. It is electric dipole allowed transition and very sensitive to coordination environment of central metal ion. Therefore ratio of intensities between transitions $^5D_0 \rightarrow {}^7F_2$ and $^5D_0 \rightarrow {}^7F_1$ shows the nature and symmetry of the first coordination sphere of Eu^{3+} organic complexes. For all complexes in MeCN solutions and solid-state the intensity ratio between these two transitions is extremely high meaning that, strong coordination interactions are present in complexes **C1**-**C6** and Eu^{3+} occupies site without inversion symmetry. Moreover, the higher is the intensity ratio, the more intense is the red emission from the complex [25]. CIE chromaticity coordinates for complexes **C1**-**C6** (Table 3) calculated from their emission spectra are situated in explicit red region and completely corresponds to standard red color of NTSC (x=0.67; y=0.33) therefore being a promising candidates for application in OLEDs. Similar CIE coordinates with 100% red color purity were reported for Eu *tetrakis* complex with butyl-methoxy-dibenzoyl-methane ligands and NH_4^+ as counterion [26].

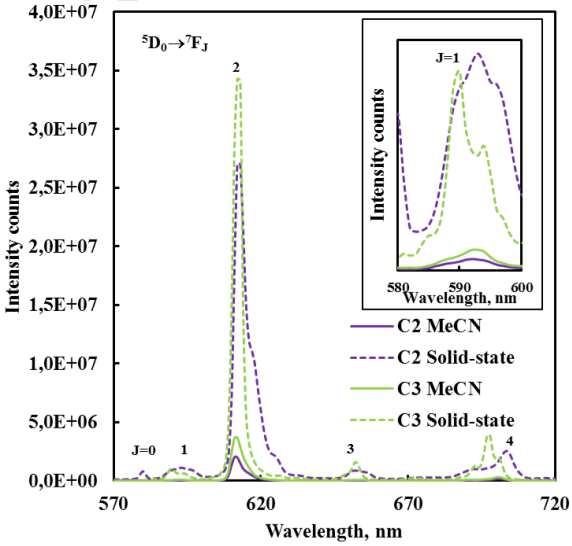

Fig. 6. Emission spectra of Eu^{3+} complexes **C2** and **C3** in MeCN solutions (c~$1.5 \cdot 10^{-5}$M) (λ_{exc}=350 nm) and solid-state (λ_{exc}=425 nm). Inset shows splitting of $^5D_0 \rightarrow {}^7F_1$ transition in the solid-state.

Furthermore, Fig. 6 also shows, that emission spectra shape is slightly affected by the complex structure. For, *ternary* complex **C2** emission band at 611 nm are much wider and shows shoulders at 615 and 625 nm. However, the same band of *tetrakis* complex **C3** exhibit one sharp line. Eu^{3+} ion *ternary* complexes with PHEN as secondary ligand usually display splitting of $^5D_0 \rightarrow {}^7F_2$ transition [8, 27], which could be explained with less ordered environment around central metal ion than in *tetrakis* complexes [19, 28].

To further establish the efficiency of the emission from complexes in MeCN solutions and in solid-state, absolute photoluminescence quantum yields (PLQY) were determined using integrating sphere. The data are shown in Table 3. Two relationships can be seen from PLQY:

(**1**) PLQY in solid state for all complexes shows higher values, than in MeCN solutions. Lower PLQY in solutions of Eu^{3+} organic complexes arise from undesirable, high frequency CH vibrational oscillators of solvent (MeCN) molecules in the surrounding environment of the complex, which effectively lowers the emission transition probabilities of central metal ion [29]. PLQY of complexes **C1**-**C3**,**C5**,**C6** were also measured in THF and $CHCl_3$ solutions and again low values (~0.01) were obtained. It is possible, that some dissociation processes of complexes are present in solutions. It is known, that in non-polar solvents *tetrakis* complexes dissociate into corresponding *tris*-complexes (for example $Eu(BID)_3$) and a β-diketonate salt (for example, $BID^-N^+(Et)_4$) [30]. First coordination sphere of Eu^{3+} ion is not fulfilled in *tris*-complexes, therefore, for Eu^{3+} to obtain coordination number 8 two solvent molecules are attached to metal. Having high frequency CH vibrational oscillators in first coordination sphere greatly lowers emission intensity and PLQY of Eu^{3+} complexes.

(**2**) In MeCN and solid-state *ternary* complexes **C1**,**C2** show lower PLQY than their analogues *tetrakis* complexes **C3-C6**. In MeCN solutions differences in PLQY between *ternary* and *tetrakis* complexes are insignificant due to low emission intensity. However, in solid-state PLQY for *tetrakis* complexes **C3** and **C4** are five to six times higher than for *ternary* complexes **C1**, **C2** and almost three to six times higher than for *tetrakis* complexes **C5**, **C6**. *Tetrakis* complexes usually are characterized with higher intensity of emission compared to analogue *ternary* complexes [6] due to due to larger cross section of photon absorption. Furthermore, in *tetrakis* complexes Eu^{3+} ion is fenced by four coordinated benzoyl-1,3-indandione ligands, which provides better shielding from surrounding environment than for *ternary* complexes.

The luminescence decay of Eu^{3+} emission related to $^5D_0 \rightarrow {}^7F_2$ (611 nm) transition of complexes **C1-C6** were determined in solid-state under pulsed laser excitation at 408 or 425 nm. The obtained lifetime values (τ_1 and τ_2) are listed in Table 3. All decay curves were fitted by bi-exponential functions and have two lifetime components τ_1 and τ_2, indicating on the presence of two sites of symmetry around the Eu^{3+}. Usually Eu^{3+} complexes with two lifetime components exhibits broadening of transition $^5D_0 \rightarrow {}^7F_0$ at emission spectra [27, 31], which also points to two sites of symmetry around central metal ion. All complexes **C1-C6** in solid-state shows slightly broad, featureless band at 580 nm, which attributes to $^5D_0 \rightarrow {}^7F_0$ transition. Different symmetry around Eu^{3+} ions probably forms from different distances between emitting Eu^{3+} ions in the solid-state. When distance between two emitting Eu^{3+} ion sites are short, some interactions between Eu^{3+}- Eu^{3+} centers take place, which could lead to two different chemical environment formation around Eu^{3+}

ions. Longest decay lifetimes were obtained for *tetrakis* complexes with $N^+(Et)_4$ cation and are 233 and 54 µs for **C3** and 203 and 118 µs for **C4**.

From obtained PLQY and lifetime values, we can draw a conclusion, that the used countercation ($N^+(Et)_4$ or $N^+(Bu)_4$) affects emission properties of synthesized complexes more than complex structure in solid-state. For ternary complexes **C1**, **C2** and *tetrakis* complexes **C5**, **C6** with $N^+(Bu)_4$ cation obtained PLQY and lifetime values were close. However, complexes with $N^+(Et)_4$ as counteraction exhibits three (BID ligand) or even six times (MBID) higher PLQY values than their analogues with $N^+(Bu)_4$ cation. Such difference in emission efficiency could be as a result of different cation incorporation in the crystal structure of complex in solid-state. Therefore, in MeCN solutions, where these long-range order is absent and complex exist as anion ($[Eu(BID)_4]^-$; $[Eu(MBID)_4]^-$) no difference in PLQY were observed. In solid-state counter cation size is the mayor factor, which influences the emission properties as it was shown in the report [9]. Increase in the counteraction size usually decrease complex emission efficiency and emission data of our newly synthesized complexes confirms this statement.

3.6. Photoluminescence from polymer films doped with Eu^{3+} complexes

The mayor drawback for practical application of Eu^{3+} organic complexes are their poor carrier-transporting ability and film formability. Therefore, to overcome this problem, complexes need to be doped in host materials, which could provide missing properties, for example, in polymers. Two polymers – *N*-polyvinylcarbazole (PVK) and poly methyl methacrylate (PMMA) were chose as host materials for our complexes. PVK owing excellent hole transporting properties as well as good match between its triplet energy state and energy levels of most Eu^{3+} β-diketone complexes

is one of the most used host materials for metal organic complexes. However, PMMA was chosen due to its low optical absorbance (it is transparent at wavelengths >250 nm). The doping mass of polymer films was chosen 8 wt%, according to our [32] and other authors [11, 24, 33, 34] reported investigations about relationship of doping mass – emission efficiency of doped PVK and PMMA films with Eu^{3+} complexes. Lower doping mass (0.5-2 wt%) could lead to incomplete energy transfer between host and doping complex, however, high doping mass (>12 wt%) could lead to non-radiative energy transfer between two metal ions (Eu^{3+}-Eu^{3+}), which decreases emission intensity of doped films. PVK and PMMA polymer films doped with 8 wt% of Eu^{3+} complexes were prepared by spin-coating technique from THF solutions (due to complex **C4** low solubility in commonly used solvents, PVK film with 8 wt% of **C4** wasn't prepared, but PMMA film was obtained from MeCN solution). UV/VIS absorption spectra of prepared films are depicted in Fig.7 (**A**) and Fig. 8 (**A**).

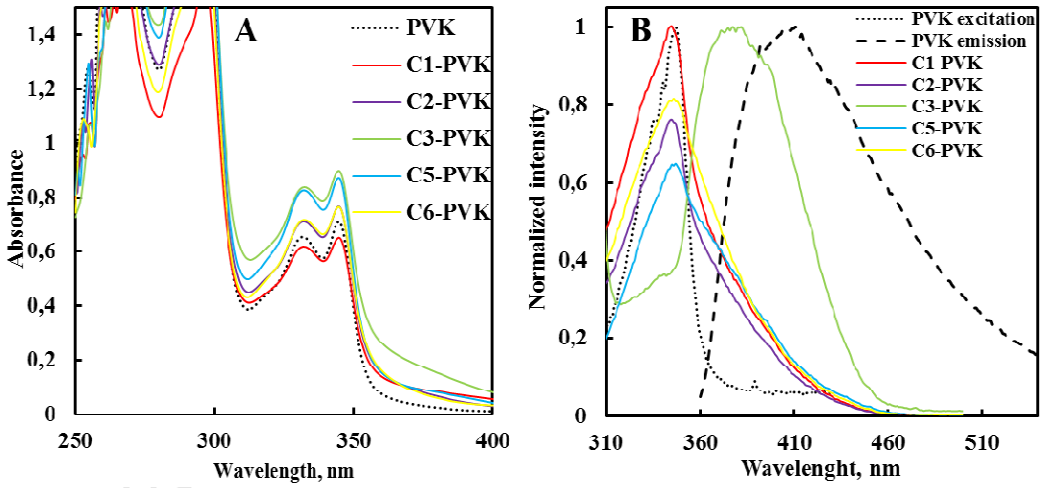

Fig. 7. (**A**) – UV/Vis absorption spectra of pure PVK film and PVK films containing 8 wt% of Eu^{3+} complexes **C1-C3**,**C5**,**C6**; (**B**) - Excitation spectra ($\lambda_{mon\ PVK}$=435 nm) and emission spectra (λ_{exc}=346 nm) of pure PVK film and excitation spectra of PVK films containing 8 wt% of Eu^{3+} complexes **C1-C3**,**C5**,**C6** (λ_{mon} =611 nm).

UV/Vis spectra of pure PVK film exhibit broad absorption in 250-350 nm range, with $\lambda_{abs\ max}$ at 271, 297, 327 and 348 nm, which can be assigned to π-π* and n-π* transitions of *N*-polyvinylcarbazole. Nevertheless, absorption profile of doped

559 PVK films exhibits the same profile as pure thin film, which appoints to absorption
560 overlap between host matrix and Eu^{3+} complexes. However, in the spectral region
561 from 350 to 400 nm new absorption band arises for doped PVK films and can be
562 attributed to the absorption of ligands (BID, MBID). This band is particular
563 pronounced for *tetrakis* complex **C3**, which also showed red-shift of excitation
564 spectra in solid-state, compared to other complexes. Completely different situation is
565 found for doped PMMA films (Fig. 8 (**A**)). These films exhibit pure complex
566 absorption profile with two $\lambda_{abs\ max}$ at ~ 297 nm and ~ 337 nm (Table 4), which
567 compared to $\lambda_{abs\ max}$ in MeCN solutions are shifted to longer wavelengths.

568 Excitation spectra of pure PVK film (Fig. 7 (**B**)) (λ_{mon}=435 nm) shows sharp
569 band (300-360 nm) with maximum at 346 nm and corresponding doping films
570 (λ_{mon}=611 nm) with complexes **C1**,**C2**,**C5**,**C6** exhibits the same maximum, but
571 excitation bands shows shoulder at longer wavelengths rising from 360 to 420 nm.
572 Only polymer film doped with *tetrakis* complex **C3** shows distinct excitation spectra
573 from pure PVK film (350-460 nm with λ_{exc}= 379 nm). Furthermore, all excitation
574 spectra of PVK films doped with complexes **C1**-**C3**,**C5**,**C6** slightly overlaps with
575 emission spectra of PVK (355-550 nm) (Fig 7 (**B**)), which could also be advantageous
576 for polymer films due to fact, that host would provide additional excitation energy for
577 complex, therefore increasing emission efficiency. From these excitation spectra we
578 can conclude, that PVK films can be excited not only through $\pi \rightarrow \pi^*$ transitions of the
579 ligands, but also through host matrix transitions.

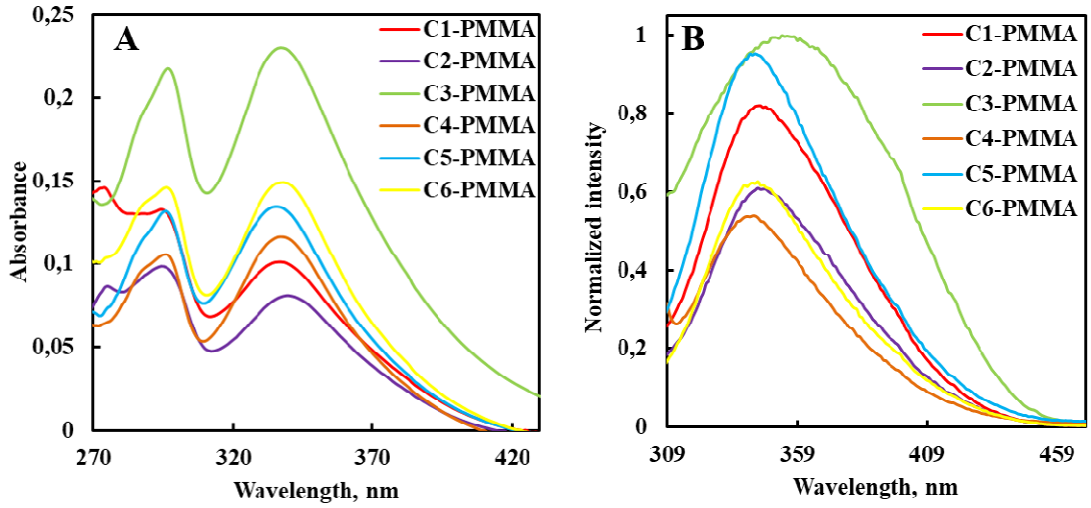

Fig. 8. (**A**) – UV/Vis absorption spectra of PMMA films containing 8 wt% of Eu^{3+} complexes **C1-C6**; (**B**) – Excitation spectra of PMMA films containing 8 wt% of Eu^{3+} complexes **C1-C6** (λ_{mon} =611 nm).

Furthermore, excitation spectra of PMMA films (Fig. 8. (**B**)) reveal wide bands in the range from 309 to 450 nm, with λ_{exc} ~347 nm. Excitation spectra very well corresponds to absorption spectra, meaning that these bands can be attributed to $\pi \rightarrow \pi^*$ transitions of coordinated ligands. Slight shift of λ_{abs} and λ_{exc} in PMMA matrices compared to ones in MeCN solution, points out to some interactions between ligands from complexes **C1-C6** and PMMA matrix.

Table 4

Optical properties of PVK and PMMA films doped with 8 wt% of complexes **C1-C6**.

	PVK films					PMMA films				
	λ_{abs}, nm	λ_{exc}, nm	τ_1, µs	τ_2, µs	PLQY[b]	λ_{abs}, nm	λ_{exc}, nm	τ_1, µs	τ_2, µs	PLQY[c]
C1	332, 345	344	47±0.5 (92%)	179±3 (8%)	0.04	337	347	75±1 (83%)	306±8 (17%)	0.12
C2	332, 345	345	50±0.7 (95%)	193±7 (5%)	0.04	341	347	74±1 (90%)	317±14 (10%)	0.11
C3	332, 345	377	60±1 (95%)	199±14 (5%)	0.08	337	353	56±0.6 (85%)	204±2 (15%)	0.14
C4	-[a]	-[a]	-[a]	-[a]	-[a]	339	342	68±1 (88%)	256±7 (12%)	0.10
C5	332, 345	347	40±0.5 (94%)	139±2 (6%)	0.05	336	342	72±1 (85%)	255±6 (15%)	0.14
C6	332, 345	346	42±0.8 (97%)	154±9 (3%)	0.04	339	345	53±0.6 (88%)	214±2 (12%)	0.09

[a-] Film wasn't obtained due to complex **C4** low solubility in THF, $CHCl_3$;
[b-] PLQY determined with λ_{exc}=370 nm;
[c-] PLQY determined with λ_{exc}=340 nm;

595 Emission spectra of doped polymer films are shown in Fig. 9. All five PVK
596 films shows characteristic Eu^{3+} ion emission lines, also no emission from matrix
597 (PVK) in the range from 360 to 520 nm are observed indicating, that complete energy
598 transfer process between host and complexes are present in these films. PLQY were
599 determined using two excitation wavelengths. First, doped films were excited with
600 350 nm (through host matrix transitions) and obtained PLQY values were low (0.03-
601 0.04). Second, doped PVK films were excited with 370 nm (through coordinated
602 ligands transitions) and obtained PLQY were higher (0.04-0.08) (Table 4) indicating,
603 that direct excitation through complex absorption region is more efficient, than
604 through host matrix absorption region. Similar to emission properties in MeCN
605 solutions and in solid-state, highest quantum yield was obtained for *tetrakis* complex
606 **C3** with $N^+(Et)_4$ countercation, due to fact, that its excitation spectra show the largest
607 overlap with host matrix emission spectra, which increases the efficiency of energy
608 transfer process between host and doping substance. The obtained PLQY of doped
609 PVK films are lower than other reported doped PVK films with ternary complexes
610 [35].

611 Furthermore, all six PMMA doped films exhibit more intense red light
612 emission (Fig. 9 (**B**)) with much higher quantum yields (0.09-0.14) than for PVK
613 films confirming the assumption, that one of the main factors why PVK films showed
614 low PLQY are undesirable absorption spectra overlap between matrix and complex.
615 Yet again the highest PLQY were obtained for *tetrakis* complexes **C3** and **C5** – 0.14.
616 The obtained PLQY of doped PMMA films are close or slightly lower than other
617 reported doped PMMA films containing Eu complexes with rigid β-diketones [11].

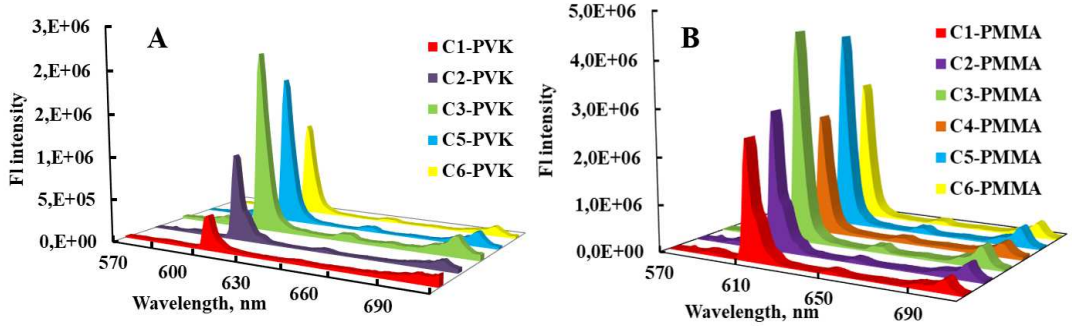

Fig. 9. (**A**) - Emission spectra of PVK films containing 8 wt% of Eu^{3+} complexes **C1-C3**,**C5**,**C6**; (**B**) - Emission spectra of PMMA films containing 8 wt% of Eu^{3+} complexes **C1-C6**.

The luminescence decay curves for all PVK and PMMA doped films were found to be bi-exponential and relevant time components τ_1 and τ_2 are given in Table 4. As it seems, both luminescence lifetime values for doped films are longer than it was in the solid-state and can be explained with greater distance between two emitting centers Eu^{3+}-Eu^{3+} in polymer films, which reduces possibility of energy transfer between Eu^{3+}-Eu^{3+} as a non-radiative process. Two lifetime components τ_1 and τ_2 for polymer films could be connected with complex interaction with hosts, which could lead to two different emitting sites – one being unbounded complex, other – complex bounded with polymers PMMA and PVK. Similar conclusions were reported for $Eu(DBM)_3PHEN$ complex doped in PMMA matrix [21].

Herein we conclude, that PMMA matrix provides excellent, transparent film formability for Eu^{3+} organic complexes with no influence on absorption or properties of doping complex. Obtained films exhibit moderate PLQY and lifetime values and could show potential in application as polymer optical fibers, which are being used in luminescent solar concentrators and luminescent biosensors.

4. CONCLUSIONS

Structures of newly synthesized *ternary* and *tetrakis* Eu^{3+} complexes $Eu(BID)_3(PHEN)$, $Eu(MBID)_3(PHEN)$, $[Eu(BID)_4]^-N^+(Et)_4$, $[Eu(MBID)_4]^-N^+(Et)_4$,

$[Eu(BID)_4]^-N^+(Bu)_4$ and $[Eu(MBID)_4]^-N^+(Bu)_4$ were neatly characterized with elemental analysis, ^{1}H-NMR spectroscopy, mass spectroscopy, FT-IR spectra and X-Ray diffraction analysis. Complex structure (*ternary* or *tetrakis*) did not affect excitation window (300 to 450 nm) and CIE chromaticity coordinates (x=0.670; y=0.330) for emission spectra in the solid-state and solution. However, complex structure greatly affects thermal properties and emission properties in the solid-state *Tetrakis* complexes with structure $[Eu(BID)_4]^-N^+(Et)_4$ and $[Eu(MBID)_4]^-N^+(Et)_4$ showed higher PLQY values (0.29 and 0.60) than corresponding *ternary* complexes (0.06-0.10) in the solid-state. Countercation ($N^+(Et)_4$ or $N^+(Bu)_4$) size noticeably affects emission properties of *tetrakis* complexes. Increase in the countercation size decrease complex emission efficiency. For each complex two polymer films (PVK and PMMA) with doping mass of 8 wt% were prepared and optical properties investigated. Highest PLQY (0.09-0.14) and longest lifetime values (τ_1=53-74 µs; τ_2=203-316 µs) were obtained for doped PMMA films. Obtained PMMA films could show potential in application as polymer optical fibers or in polymer organic light emitting diodes.

ACKNOWLEDGEMENTS

This work was supported by the doctoral studies grant of Riga Technical University (Grant Nr. 34-14000DOK.MLĶF/17) and the National Research Program of Latvia “IMIS2”.

SUPPLEMENTARY MATERIAL

The deposition number CCDC 1843401 for complex **C4** contains the supplementary crystallographic data for this paper. These data can be obtained free of charge at www.ccdc.cam.ac.uk/data_request/cif or from the Cambridge

Crystallographic Data Centre (CCDC), 12 Union Road, Cambridge CB2 1EZ, UK; fax: +44 (0) 1223 336033; email:deposit@ccdc.cam.ac.uk.

REFERENCES

[1] Syamchand SS, Sony G. Europium enabled luminescent nanoparticles for biomedical applications. J Lumin 2015;165:190–215. https://doi.org/10.1016/j.jlumin.2015.04.042

[2] Carlos LD, Ferreira RAS, de Zea Bermudez V, Ribeiro SJL. Lanthanide-Containing Light-Emitting Organic–Inorganic Hybrids: A Bet on the Future. Adv Mater 2009;21:509–34. https://doi.org/10.1002/adma.200801635

[3] Gao R, Zhao M, Guan Y, Fang X, Li X, Yan D. Ordered and flexible lanthanide complex thin films showing up-conversion and color-tunable luminescence. J Mater Chem C 2014;2:9579-86. http://dx.doi.org/10.1039/C4TC01213E

[4] **Yang X, Lin X, Zhao Y, Zhao YS, Yan D. Lanthanide Metal–Organic Framework Microrods: Colored Optical Waveguides and Chiral Polarized Emission. Angew Chem Int Ed 2017;56:7853–57.** https://doi.org/10.1002/anie.201703917

[5] Liu Y, Wang Y, Li C, Huang Y, Dang D, Zhu M, Zhu W, Cao Y. Red polymer light-emitting devices based on an oxadiazole functionalized europium(III) complex. Mater Chem Phys 2014;143:1265-70. http://dx.doi.org/10.1016/j.matchemphys.2013.11.032

[6] Binnemans, K. Lanthanide-Based Luminescent Hybrid Materials. Chem Rev 2009;**109**:4283-374.

[7] Cotton S. Lanthanide and Actinide Chemistry. England: John Wiley & Sons; 2006. http://dx.doi.org/10.1002/0470010088

[8] Lunstroot K, Driesen K, Nockemann P, Viau L, Mutin PH, Vioux A, Binnemans K. Ionic liquid as plasticizer for europium(III)-doped luminescent poly(methyl methacrylate) films. Phys Chem Chem Phys 2010;12:1879–85. http://dx.doi.org/10.1039/B920145A

[9] Mech A, Karbowiak M, Görller-Walrand C, Van Deun R. The luminescence properties of three tetrakis dibenzoylmethane europium(III) complexes with different counter ions. J Alloys Compd 2008:451:215–19. https://doi.org/10.1016/j.jallcom.2007.05.019

[10] Li J, Li H, Yan P, Chen P, Hou G, Li G. Synthesis, Crystal Structure, and Luminescent Properties of 2-(2,2,2-Trifluoroethyl)-1-indone Lanthanide Complexes. Inorg Chem 2012;51:5050−57. http://dx.doi.org/10.1021/ic202473b

[11] Li W, Yan P, Hou G, Li H, Li G. Efficient red emission from PMMA films doped with 5,6-DTFI europium(III) complexes: synthesis, structure and photophysical properties. Dalton Trans 2013;42:11537-47. http://dx.doi.org/10.1039/C3DT50580D

[12] Teotonio EES, Brito HF, Cremona M, Quirino WG, Legnani C, Felinto MCFC., Novel electroluminescent devices containing Eu3+-(2-acyl-1,3-indandionate) complexes with TPPO ligand. Opt Mater 2009;32:345–49. http://dx.doi.org/10.1016/j.optmat.2009.08.015

[13] Teotonio EES, Brito HF, Viertler H, Faustino WM, Malta OL, de Sá GF, et al. Synthesis and luminescent properties of Eu^{3+}-complexes with 2-acyl-1,3-indandionates (ACIND) and TPPO ligands: The first X-ray structure of Eu–ACIND complex. Polyhedron 2006;25:3488–94. http://dx.doi.org/10.1016/j.poly.2006.06.035

712 [14] Altomare A, Burla M, Cammali M, Cascarano G, Giacovazzo C, Guagliardi A,
713 Moliterni A, Spagna. SIR97: A New Tool for Crystal Structure Determination and
714 Refinement. J Appl Cryst 1999;32:115-9.
715 http://dx.doi:10.1107/S0021889898007717
716 [15] Sheldrick GM. A short history of *SHELX*. Acta Cryst 2008;A64:112-22.
717 http://dx.doi.org/ 10.1107/S0108767307043930
718 [16] Mackay S, Dong W, Edwards C, Henderson A, Gilmore CJ, Stewart N,
719 Shankland K, Donald A. maXus, Integrated Crystallography Software, 2003, Bruker-
720 Nonius and University of Glasgow.
721 [17] Wang N, Tao X, Du FL, Feng M, Jiang LN, Shen YZ. Synthesis and
722 characterization of organophosphine/phosphite stabilized silver(I) complexes bearing
723 2-acetyl-1,3-indandione ligand, crystal structure of [$Ph_3P{\cdot}AgC_{11}H_7O_3$], Polyhedron
724 2010;29:1687–91. http://dx.doi.org/doi:10.1016/j.poly.2010.02.017
725 [18] Biju S, Freire RO, Eom YK, Scopelliti R, Bunzli JCG, Kim HK. A Eu^{III} Tetrakis
726 (β-diketonate) Dimeric Complex: Photophysical Properties, Structural Elucidation by
727 Sparkle/AM1 Calculations, and Doping into PMMA Films and Nanowires. Inorg
728 Chem, 2014;53:8407-17. http://dx.doi.org/10.1021/ic500966z
729 [19] Malba CM, Enrichi F, Facchina M, Demitri N, Plaisier JR, Natile MM, Selva M,
730 Riello P, Perosa A, Benedetti A. Phosphonium-based tetrakis dibenzoylmethane
731 Eu(III) and Sm(III) complexes: synthesis, crystal structure and photoluminescence
732 properties in a weakly coordinating phosphonium ionic liquid. RSC Adv 2015;5:
733 60898-907. http://dx.doi.org/10.1039/C5RA03947A
734 [20] Sweeting LM, Rheingold AL. Crystal disorder and triboluminescence:
735 triethylammonium tetrakis(dibenzoylmethanato)europate. J Am Chem Soc
736 1987;109:2652–58. http://dx.doi.org/10.1021/ja00243a017

[21] Singh AK, Singh SK, Mishra H, Prakash R, Rai SB. Structural, Thermal, and Fluorescence Properties of $Eu(DBM)_3Phen_x$ Complex Doped in PMMA. J Phys Chem B 2010;114:13042–51. http://dx.doi.org/10.1021/jp1050063

[22] Biju S, Xu LJ, Sun CZ, Chen ZN. White OLEDs Based on a novel Eu^{III}-Tetrakis-β-Diketonate Doped into 4,4'-N,N'-Dicarbazlebiphenyl as Emitting Material. J Mater Chem C 2015;3:5775-82. http://dx.doi.org/10.1039/C5TC00638D

[23] Zhou D, Huang C, Yaong G, Bai J, Li T. Luminescent europium dibenzoylmethane complexes and their Langmuir-Blodgett films. J Alloys Compd 1996;235:156-62. https://doi.org/10.1016/0925-8388(95)02159-0

[24] Raj DBA, Francis B, Reddy MLP, Butorac RR, Lynch VM, Cowley AH. Highly Luminescent Poly(Methyl Methacrylate)-Incorporated Europium Complex Supported by a Carbazole-Based Fluorinated β-Diketonate Ligand and a 4,5-Bis(diphenylphosphino)-9,9-dimethylxanthene Oxide Co-Ligand. Inorg Chem 2010;49:9055–63. http://dx.doi.org/10.1021/ic1015324

[25] Binnemans K. Rare-earth beta-diketonates. Handbook on the Physics and Chemistry of Rare Earths Vol. 35, North Holland:Elsevier; 2005.

[26] Adati RD, Lima SAM, Davolos MR, Jafelicci M. A new β-diketone complex with high color purity, J Alloys Compd 2006;418:222–25. https://doi.org/10.1016/j.jallcom.2005.10.062

[27] Malina I, Kampars V, Photoluminescent properties of novel tris, ternary and tetrakis Eu(III) organic complexes with 2-acetyl-1,3-indandione ligands, Materials, Methods & Technologies, 2017;17:18-27.

[28] Seo SJ, Zhao D, Suh K, Shin JH, Bae BS. Synthesis and luminescence properties of mesophase silica thin films doped with in-situ formed europium complex. J Lumin 2008;128:565–572. https://doi.org/10.1016/j.jlumin.2007.08.012

762 [29] Ahmed Z, Iftikhar K. Efficient Layers of Emitting Ternary Lanthanide
763 Complexes for Fabricating Red, Green, and Yellow OLEDs. Inorg Chem
764 2015;54:11209-25. http://dx.doi.org/10.1021/acs.inorgchem.5b01630
765 [30] Gao R, Koeppen C, Zheng G, Garito AF. Effects of chromophore dissociation on
766 the optical properties of rare-earth-doped polymers. Appl Opt 1998;37:7100-06.
767 https://doi.org/10.1364/AO.37.007100
768 [31] Liu HG, Park S, Jang K, Zhang WS, Seo HJ, Lee YI. Different photoluminescent
769 properties of binary and ternary europium chelates doped in PMMA, Mater Chem
770 Phys 2003;82:84–92. https://doi.org/10.1016/S0254-0584(03)00216-5
771 [32] Malina I, Juhnevics N, Kampars V. Study of thermal and optical properties of
772 dibenzoyl-methane Eu(III) organic complexes. P Est Acad Sci 2017;66:493-500.
773 http://dx.doi.org/10.3176/proc.2017.4.11
774 [33] Zhang Y, Li C, Shi H, Du B, YangW, Cao Y. Bright red light-emitting
775 devices based on a novel europium complex doped into polyvinylcarbazole. New J
776 Chem 2007;31:569–74. http://dx.doi.org/10.1039/B617612G
777 [34] Deichmann VAF, Novo JBM, Cirpan A, Karasz FE, Akcelrud L. Photo-and
778 Electroluminescent behaviour of Eu^{3+} Ions in Blends with Poly(vinyl-carbazole). *J*
779 *Braz Chem Soc* 2007;18:330-36. http://dx.doi.org/10.1590/S0103-
780 50532007000200013
781 **[35] Knyazev AA, Krupin AS, Romanova KA, Galyametdinov YG.**
782 **Luminescence and energy transfer in poly(Nvinylcarbazole) blends doped by a**
783 **highly anisometric Eu(III) complex.** J Coord Chem 2016;69:1473-83.
784 https://doi.org/10.1080/00958972.2016.1185781

Highlights

New ternary and tetrakis Eu^{3+} complexes with 2-benzoylindandione ligands are reported.

Tetrakis complexes exhibit more intense emission than analogue ternary complexes.

Counterion size of tetrakis complexes greatly affects quantum yield in solid state.

Doped PMMA films with Eu^{3+} complexes have higher quantum yields than doped PVK films.

Synthesized Eu^{3+} complexes show potential application in photonic devices.